International Journal of Engineering, Mathematical and Physical Sciences
ISSN: 2517-9934
Vol:3, No:2, 2009

An Overview of Some High Order and Multi-Level Finite Difference Schemes in Computational Aeroacoustics

Appanah Rao Appadu, and Muhammad Zaid Dauhoo

***Abstract*—**In this paper, we have combined some spatial derivatives with the optimised time derivative proposed by Tam and Webb in order to approximate the linear advection equation which is given by $\frac{\partial u}{\partial t}+\frac{\partial f}{\partial x}=0$. These spatial derivatives are as follows: a standard 7-point 6^{th}-order central difference scheme (ST7), a standard 9-point 8^{th}-order central difference scheme (ST9) and optimised schemes designed by Tam and Webb, Lockard et al., Zingg et al., Zhuang and Chen, Bogey and Bailly. Thus, these seven different spatial derivatives have been coupled with the optimised time derivative to obtain seven different finite-difference schemes to approximate the linear advection equation. We have analysed the variation of the modified wavenumber and group velocity, both with respect to the exact wavenumber for each spatial derivative. The problems considered are the 1-D propagation of a Boxcar function, propagation of an initial disturbance consisting of a sine and Gaussian function and the propagation of a Gaussian profile. It is known that the choice of the *cfl* number affects the quality of results in terms of dissipation and dispersion characteristics. Based on the numerical experiments solved and numerical methods used to approximate the linear advection equation, it is observed in this work, that the quality of results is dependent on the choice of the *cfl* number, even for optimised numerical methods. The errors from the numerical results have been quantified into dispersion and dissipation using a technique devised by Takacs. Also, the quantity, Exponential Error for Low Dispersion and Low Dissipation, **eeldld** has been computed from the numerical results. Moreover, based on this work, it has been found that when the quantity, **eeldld** can be used as a measure of the total error. In particular, the total error is a minimum when the **eeldld** is a minimum.

***Keywords*—**Optimised time derivative, dissipation, dispersion, *cfl* number.

Nomenclature: k : time step; h : spatial step; β : advection velocity; r: *cfl*/Courant number; $r=\frac{\beta k}{h}$; $w=\theta h$: exact wave number; n : time level; *RPE* : Relative phase error per unit time step; *AFM* : modulus of amplification factor.

A. R. Appadu is a PhD student at the University of Mauritius, Mauritius (e-mail: biprao2@yahoo.com).

M. Z. Dauhoo (Corresponding author) is a Senior Lecturer at the University of Mauritius, Mauritius (e-mail: m.dauhoo@uom.ac.mu).

I. Introduction

COMPUTATIONAL aeroacoustics (CAA) has been given increased interest because of the need to better control noise levels from aircrafts, trains and cars due to increased transport and stricter regulations from authorities [13]. Other applications of CAA are in the simulation of sound propagation in the atmosphere to the improved design of musical instruments [13].

The field of CAA has grown rapidly during the last decade and there has been a resurgence of interest in aeroacoustic phenomena characterised by harsher legislation and increasing environmental awareness. CAA is concerned with the accurate numerical prediction of aerodynamically generated noise as well as its propagation and far-field characteristics.

CAA involves mainly the development of numerical methods which approximate derivatives in a way that better preserves the physics of wave propagation unlike typical aerodynamic computations [13].

In this paper, we shall be concerned with problems in which low amplitude wave propagation takes place over distances characterised by large multiples of wavelength. Such problems arise in the following areas [16]:

1) Acoustics and Aeroacoustics, for noise abatement
2) Electromagnetics, for microcircuit design
3) Elastodynamics, for nondestructive testing
4) Seismology, for oil exploration
5) Medical Imaging, for accurate diagnosis
6) Hyperthermia, for noninvasive surgery

Both dissipation and dispersion errors are important. However, dissipation is more damaging to practical calculations. A wave that is excessively damped disappears and hence there is no solution to see. On the other hand, dispersion leaves the wave intact, but in the wrong place. In general, higher order schemes would be more suitable for CAA than the lower-order schemes since, overall, the former are less dissipative [11]. This is the reason why higher-order spatial discretisation schemes have gained considerable interest in computational acoustics.

Aerodynamics and other areas of fluid mechanics have benefitted immensely from the development of CFD [23]. The numerical analysis of flows around full aircraft configurations has become feasible with advances in both

numerical techniques and computing machines. The temptation to apply effective CFD methods to aeroacoustic problems has been unavoidable and has been met with some success but in some cases, it has been observed that there is a necessity for some numerical protocols specific to problems involving disturbance propagation over long distances. The difference between aerodynamic and aeroacoustic problems lies mainly in the fact that for aeroacoustic computations, the solution is desired at some large distance from the aerodynamic source but in the case of aerodynamic problems, flow properties are required accurately only on the body itself [23].

Most aerodynamics problems are time independent, whereas
aeroacoustics problems are by definition, time dependent [20]. There are computational issues that are unique to aeroacoustics. Thus, computational aeroacoustics requires somewhat independent thinking and development [20].

At specific Courant numbers and angles of propagation, the perfect-shift property can be obtained, leading to exact propagation for all wavenumbers [25]. The perfect shift property refers to the situation when the error from the spatial discretisation precisely cancels that from the temporal discretisation. Several schemes which combine the spatial and temporal discretisation produce the perfect shift property at specific Courant numbers [25]. Often this perfect cancellation of temporal and spatial errors occur at cfl 1.0. For such methods, the error increases as the cfl number is decreased and no longer cancels the spatial error. As the cfl numbers tend to zero, so does the temporal error and thus only spatial error remains. For most schemes a low cfl represents the worst case associated with large dispersion or large dissipation errors as there is no cancellation of temporal and spatial errors [25].

Thus it is important to assess numerical methods over a range of Courant numbers [25]. However, this not an issue for schemes built up from a high-accuracy spatial discretisation with a high-accuracy time-marching method. These schemes generally do not rely on cancellation to achieve high accuracy and thus the error does not increase as the Courant number is reduced.

The concept of Minimised Integrated Square Difference error, (**MISDE)** has been introduced in [1]. It mainly deals with the notion that dissipation inherent to a numerical scheme can be used to curb the prevailing dispersion optimally. The work in [2] serves as a prelude to the concept of **MISDE**. In a nutshell, **MISDE** has been used to optimise the cfl number or both the cfl number and another parameter with the aim of improving the shock capturing abilities of numerical schemes [1, 3, 4, 5].

Recently an improved technique of optimisation has been devised termed as Minimised Integrated Exponential Error for Low Dispersion and Low Dissipation, **MIEELDLD** [6]. This technique uses the notion that dissipation curbs dispersion in a numerical scheme under consideration and at the same time, the amount of dissipation and dispersion at which the optimal cfl or optimal parameter is obtained must be rather small. The concept of **MIEELDLD** enables better control over the grade and balance of dispersion and dissipation as compared to **MISDE**.

The quantities **sde**, **eeldld** denote the Square Difference Error, Exponential Error for Low Dispersion and Low Dissipation.

We now give the formulation of the two quantities which are concerned with the techniques of optimisation namely, **MISDE** and **MIEELDLD**. These are described as follows:

$ISDE = \int sde \; dw$ and $IEELDLD = \int eeldld \; dw$, where

$sde = \left(RPE - AFM\right)^2$ and

$eeldld = \exp||1 - RPE|\text{-}(1\text{-}AFM)| + \exp(|1 - RPE| + (1\text{-}AFM))\text{-}2.$

The errors from the numerical results are quantified into dissipation and dispersion according to a technique devised by Takacs [21].

The paper is organised as follows. We give a description of the spatial and temporal discretisations considered in this work. We next perform a spectral analysis of the spatial derivatives. Lastly, the results are displayed and errors are tabulated for some 1-D wave propagation problems and some concluding remarks are made.

A. Spatial and Optimised Time Discretisations

A four-level finite difference approximation of the form

$$u^{n+1} - u^n \approx k \sum_{i=0}^{3} b_i \left(\frac{dU}{dt}\right)^{n-i} \tag{1}$$

is considered for the time marching scheme.

For consistency, three of the four coefficients have been chosen so that eq. (1) is satisfied to order $(k)^3$ when both sides are expanded by Taylor series.

This yields $b_1 = -3b_0 + \frac{53}{12}$, $b_2 = 3b_0 - \frac{16}{3}$ and

$b_3 = -3b_0 + \frac{23}{12}$.

The coefficient b_0 is determined by requiring the Laplace transform of the scheme to be a good approximation to that of the partial derivative. Tam and Webb [19] obtained the value of b_0 as 2.30255809. Thus, b_1 =-2.49100760,

b_2 =1.57434093 and b_3 =-0.38589142.

The spatial derivative proposed by Tam and Webb [19], Lockard et al. [14], Zhuang and Chen [26], Bogey and Bailly [8] is approximated by

$$\frac{\partial f}{\partial x} \approx \frac{1}{h} \sum_{i=-N}^{N} a_i \; f(x + ih).$$

In the case of the spatial discretisation proposed by Zingg et al.
[24], we have

$$\frac{\partial f}{\partial x} \approx \frac{1}{h} \sum_{i=1}^{3} a_i \left(f(x+ih) - f(x-ih) \right) + \frac{1}{h} \left(d_0 f(x) + \sum_{i=1}^{3} d_i \left(f(x+ih) + f(x-ih) \right) \right).$$

We now give a description of the spatial derivatives used in the course of this work, in Tables I and II.

TABLE I
COEFFICIENTS FOR SPATIAL DERIVATIVES FOR ST7, ST8 AND THOSE DERIVED BY TAM AND WEBB [19], BOGEY AND BAILLY [8]

Coeffs	ST7	ST9	TAM	BOGEY
a_0	0	0	0	0
$a_1 = -a_{-1}$	45/60	224/280	0.770882	0.841570
$a_2 = -a_{-2}$	-9/60	-56/280	- .166705	0.244678
$a_3 = -a_{-3}$	1/60	32/840	0.020843	0.059463
$a_4 = -a_{-4}$	-	-1/820	-	-0076509

TABLE II
COEFFICIENTS FOR SPATIAL DERIVATIVES DERIVED BY LOCKARD ET AL. [14], ZINGG ET AL. [24], ZHUANG AND CHEN [26]

LOCKARD	ZINGG	ZHUANG
$a_{-4} = 0.0103902$	$a_1 = 0.75996126$	$a_{-4} = 0.0161405$
$a_{-3} = -.08466975$	$a_2 = -0.15812197$	$a_{-3} = -0.1228213$
$a_{-2} = 0.3420311$	$a_3 = 0.01876090$	$a_{-2} = 0.4553323$
$a_{-1} = 1.05268128$	$d_0 = 0.1$	$a_{-1} = -1.2492596$
$a_0 = 0.28727412$	$d_1 = -0.07638462$	$a_0 = 0.50189044$
$a_1 = 0.58616247$	$d_2 = 0.03228962$	$a_1 = 0.43993219$
$a_2 = -0.09814428$	$d_3 = -0.00590500$	$a_2 = -0.04121454$
$a_3 = 0.00966226$	-	-

B. Stability of Finite Difference Schemes

The stability of the finite difference scheme developed by Tam and Webb [19] which is 7-point in space and 4-point in time, referred to as the DRP scheme satisfies the stability condition, $r \leq 0.211$ as described in [15]. The interval $0 < w^* k < 0.41$ has been chosen in order to maintain satisfactory temporal resolution, where the term $w^* k$ is the effective angular frequency of the time marching scheme.

We have derived the amplification factor, ξ of the DRP scheme as the roots of the following equation :

$$\xi^4 - (1 + 2.30255809\, r\, A_1\, I)\, \xi^3 + (2.49100760\, r\, A_1\, I)\, \xi^2 - (1.57434093\, r\, A_1\, I)\, \xi + 0.38589142\, r\, A_1\, I = 0, \quad (2)$$

where

$$A_1 = 0.77088238\,(2\sin(\theta h)) - 0.166705904\,(2\sin(2\theta h)) + 0.02084314\,(2\sin(3\theta h)).$$

Solving eq.(2) for ξ is impossible using the Maple software. We have even tried to make use of the quartic formula developed by Lodovico Ferraria [10] to solve the equation but this has not been possible as the equation is a complicated quartic. Consequently, the stability region cannot be obtained using the Von Neumann Stability Analysis. Thus, the optimal cfl using the technique of Minimised Integrated Exponential Error for Low Dispersion and Low Dissipation Square [6] cannot be computed as an expression for the amplification factor cannot be obtained.

A study performed by Popescu and Shyy [15] show that in the case of the DRP scheme, a cfl number less than 0.21 guarantees numerical stability and negligible numerical damping.

C. Spectral Analysis of Some Spatial Schemes

Due to the difference between the physical and numerical wavenumber, some wave components propagate faster or slower than the wave speed of the original PDE [17]. This is how dispersion errors are induced. The real part of the modified wavenumber determines the dispersive error while the imaginary part determines the dissipative error [25]. Plots of the real part and imaginary part of the modified wavenumber v/s exact wavenumber for some numerical schemes have been made in [22].

A numerical method with a larger range over which the ratio of modified wavenumber to the exact wavenumber is close to one is more accurate in spectral space. This definition of accuracy is not related to the formal accuracy which is defined in terms of truncation error.
Expressions for the modified wavenumber in terms of the exact wavenumber for ST7, ST9 schemes and those proposed by Tam and Webb [19], Lockard et al. [14], Zingg et al. [24], Zhuang and Chen [26], Bogey and Bailly [8] have been computed. The plots of the real and imaginary parts of the modified wave number v/s the exact wavenumber are displayed in Figs. 1 to 4.

Figs. 1 and 3 show dispersion curves. These are often used to display the accuracy of numerical methods. The plots show how the numerical value of the wavenumber departs from the exact. The method proposed by Lockard et al. enters the upper triangle for $w \in [0.5,1.75]$ as shown in Fig.(1). This indicates that the numerical phase velocities are greater than the exact phase velocity for $w \in [0.5,1.75]$.

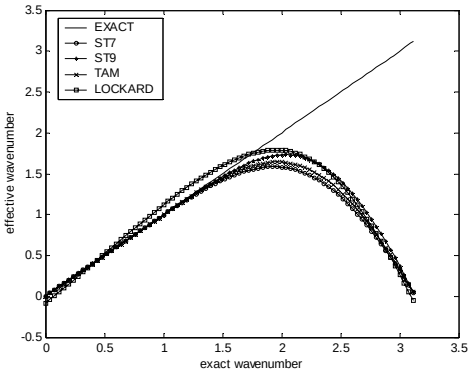

Fig. 1 Plot of real part of modified wavenumber v/s exact wavenumber for the spatial derivatives: the standard 7-pt, standard 9-pt and the schemes designed by Tam and Webb and by Lockard et al.

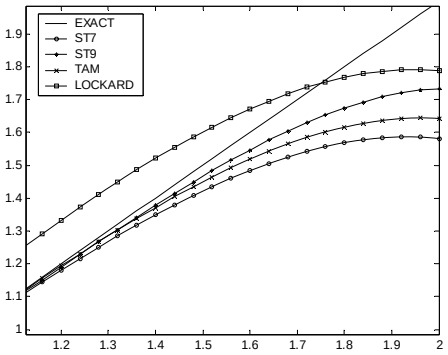

Fig. 2 Zoomed plot of Fig. 1

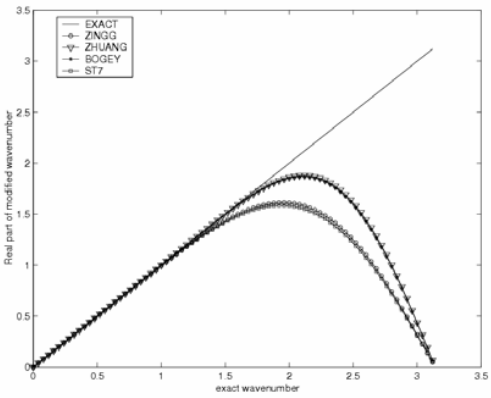

Fig. 3 Plot of real part of modified wavenumber v/s exact wavenumber for the spatial derivatives: the standard 7-pt and those designed by Zingg et al, Zhuang and Chen, Bogey and Bailly

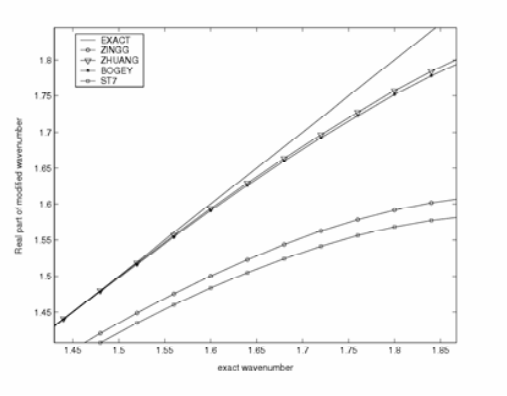

Fig. 4 Zoomed plot of Fig. 3

The imaginary part of the modified wavenumber represents numerical dissipation only when it is negative [18]. Fig.(5) shows that schemes proposed by Lockard et al., Zingg et al., Zhuang and Chen have some dissipative properties. Also, the scheme designed by Zhuang and Chen is most dissipative while the one by Zingg et al. is least dissipative. On the other hand, the spatial derivatives proposed by Tam and Webb and by Bogey and Bailly are non-dissipative.

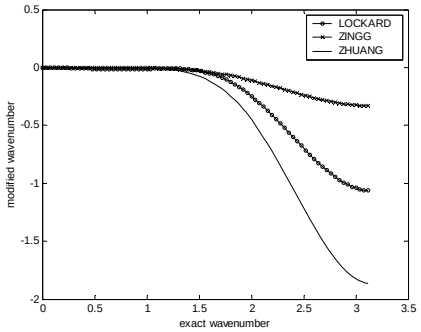

Fig. 5 Plot of imaginary part of modified wavenumber v/s exact wavenumber for spatial derivatives designed by Lockard et al, Zingg et al, and Zhuang and Chen

The group velocity of a wavepacket governs the propagation of energy of the wave packet. When the numerical wavenumber is purely real, this indicates that the scheme is non-dissipative [7]. It may also be observed that the numerical wavenumber provides a good approximation of the actual wavenumber only over a limited portion of the wavenumber spectrum. The group velocity is characterised by $\mathrm{Re}\left(\frac{d}{d(\theta h)}\left(\theta^* h\right)\right) - 1.0$ which should be almost one in order to reproduce exact result [15]. Otherwise, dispersive patterns appear. When $\mathrm{Re}\left(\frac{d}{d(\theta h)}\left(\theta^* h\right)\right) = 1.0$, the scheme has the same group velocity or speed of sound as the original governing equations and the numerical waves are propagated

with correct wave speeds.

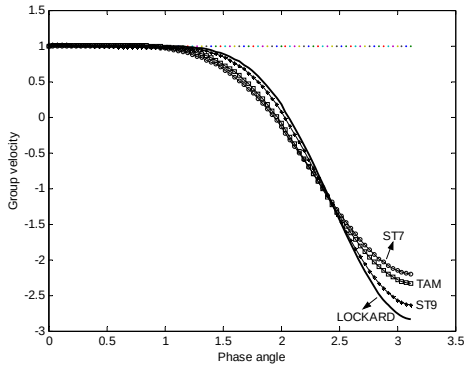

Fig. 6 Plot of group velocity v/s phase angle for the spatial derivative: stanadard 7-pt, standard 9-pt and those designed by Tam and Webb and Lockard et al

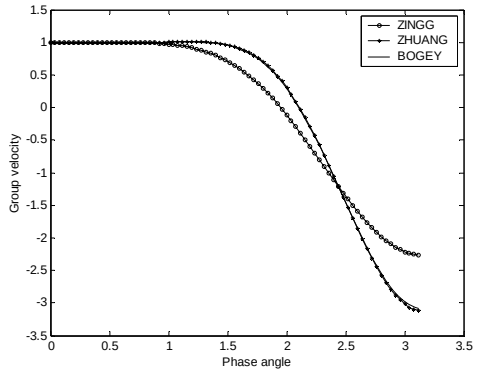

Fig. 7 Plot of group velocity v/s phase angle for the spatial derivatives designed by Zingg et al, Zhuang and Chen, Bogey and Bailly

D. 1-D Wave Propagation Problems

Propagation of Boxcar function [17]

This test problem involves discontinuous initial conditions. The initial disturbance can be written as:

$g(x) = H(x+25) - H(x-25)$, for $0 \le x \le 450$ where $H(x)$ is the Heaviside function. The Fourier transformation of $g(x)$ consists of high frequency components. These need to be damped so as to avoid spurious high frequency waves. Hence, $g(x)$ can be used to study the effect of artificial damping.

We next present the results for the spatial schemes proposed by Tam and Webb [20], Lockard et al. [14], Zingg et al. [24], Zhuang and Chen [26], Bogey and Bailly [8], all coupled coupled with the optimised time marching scheme designed by Tam and Webb, at the dimensionless time, t=400 at some different cfl numbers. Based on the numerical experiments performed, it has been found that the maximum stability limit of these schemes are 0.21, 0.21, 0.254, 0.17 and 0.22 respectively.

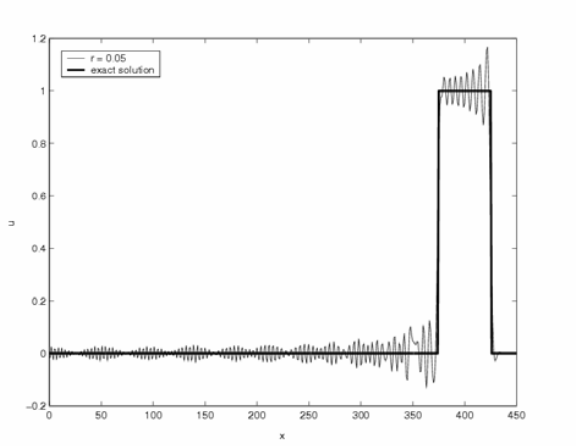

Fig. 8a Propagation of Boxcar function at dimensionless time, t=400 at cfl 0.05 using the ST7 scheme coupled with the optimised time discretisation designed by Tam and Webb

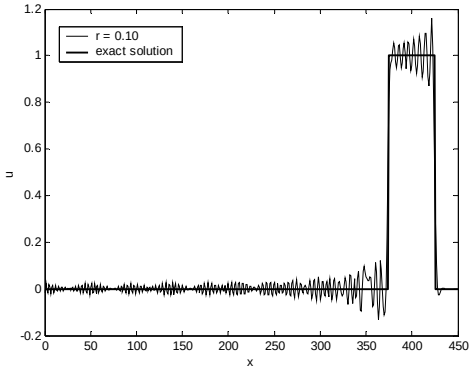

Fig. 8b Propagation of Boxcar function at dimensionless time, t=400 at cfl 0.10 using the ST7 scheme coupled with the optimised time discretisation designed by Tam and Webb

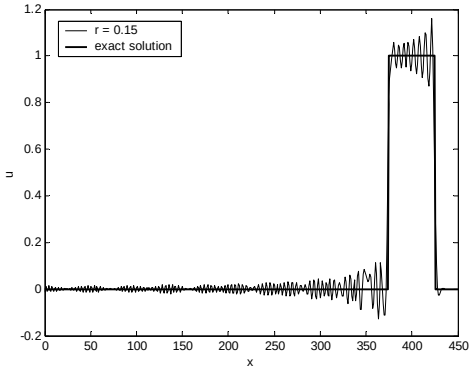

Fig. 8c Propagation of Boxcar function at dimensionless time, t=400 at cfl 0.15 using the ST7 scheme coupled with the optimised time discretisation designed by Tam and Webb

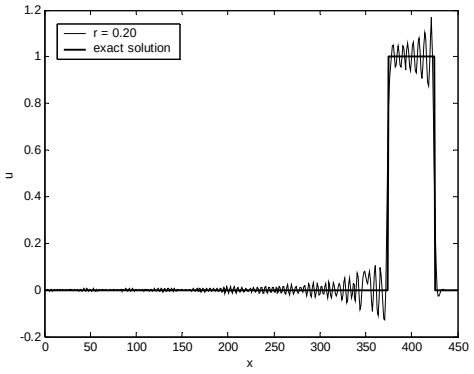

Fig. 8d Propagation of Boxcar function at dimensionless time, t=400 at cfl 0.20 using ST7 scheme coupled with the optimised time discretisation designed by Tam and Webb.

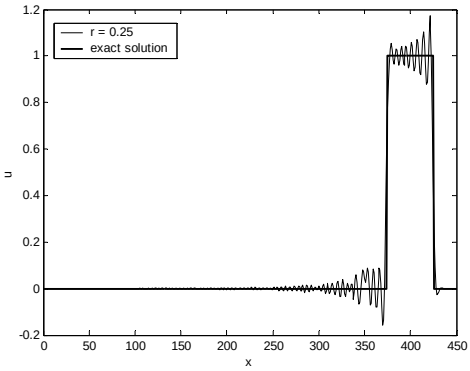

Fig. 8e Propagation of Boxcar function at dimensionless time, t=400 at cfl 0.25 using ST7 scheme coupled with the optimised time discretisation designed by Tam and Webb.

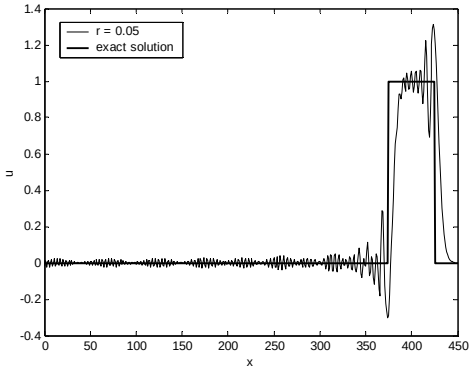

Fig. 9a Propagation of Boxcar function at a dimensionless time, t=400 at cfl 0.05 using ST9 scheme coupled with the optimised time discretisation designed by Tam and Webb.

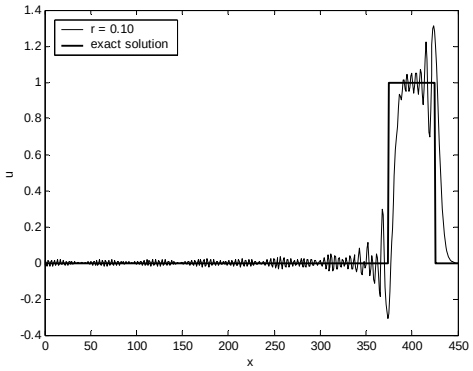

Fig. 9b Propagation of Boxcar function at a dimensionless time, t=400 at cfl 0.10 using ST9 scheme coupled with the optimised time discretisation designed by Tam and Webb.

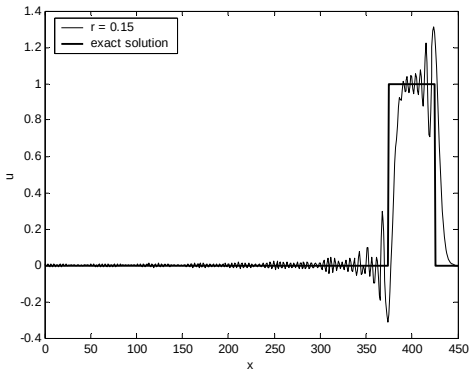

Fig. 9c Propagation of Boxcar function at a dimensionless time, t=400 at cfl 0.15 using ST9 scheme coupled with the optimised time discretisation designed by Tam and Webb.

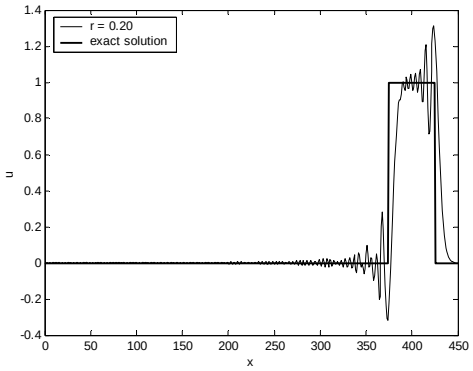

Fig. 9d Propagation of Boxcar function at a dimensionless time, t=400 at cfl 0.20 using ST9 scheme coupled with the optimised time discretisation designed by Tam and Webb.

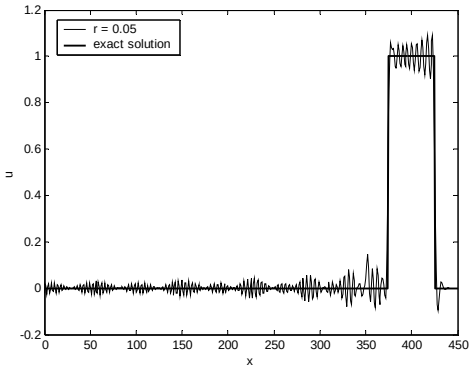

Fig. 10a Propagation of Boxcar function at dimensionless time, t=400 at cfl 0.05 using the spatial scheme coupled with the optimised time discretisation designed by Tam and Webb (DRP scheme)

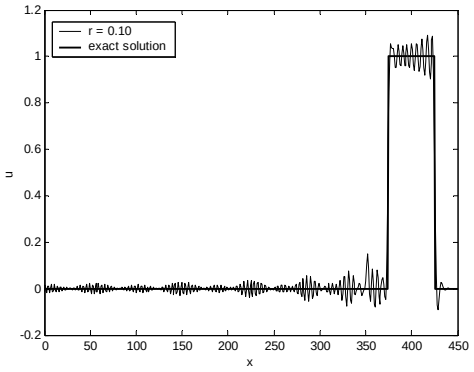

Fig. 10b Propagation of Boxcar function at dimensionless time, t=400 at cfl 0.10 using the spatial scheme coupled with the optimised time discretisation designed by Tam and Webb (DRP scheme)

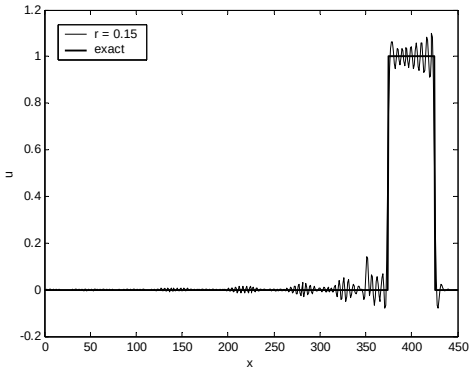

Fig. 10c Propagation of Boxcar function at dimensionless time, t=400 at cfl 0.15 using the spatial coupled with the optimised time discretisation designed by Tam and Webb (DRP scheme)

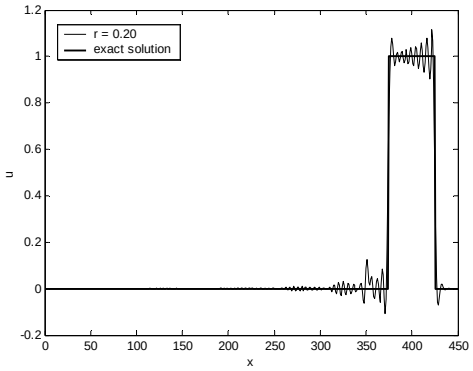

Fig. 10d Propagation of Boxcar function at dimensionless time, t=400 at cfl 0.20 using the spatial scheme coupled with the optimized time discretisation designed by Tam and Webb (DRP scheme)

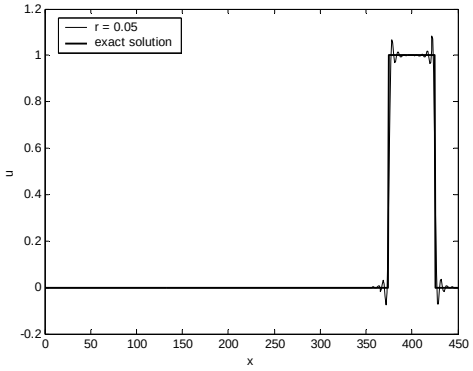

Fig. 11a Propagation of Boxcar function at dimensionless time, t=400 at cfl 0.05 using the spatial scheme proposed by Lockard et al. coupled with the optimized time discretisation designed by Tam and Webb

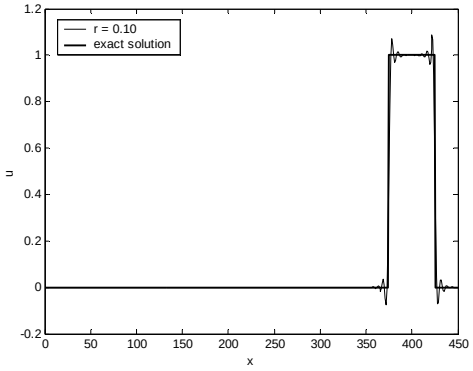

Fig. 11b Propagation of Boxcar function at dimensionless time, t=400 at cfl 0.10 using the spatial scheme proposed by Lockard et al. coupled with the optimised time discretisation designed by Tam and Webb

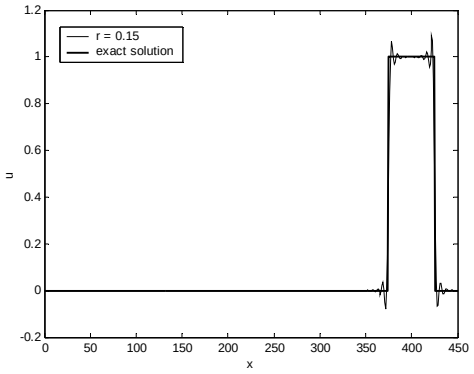

Fig. 11c Propagation of Boxcar function at dimensionless time, t=400 at cfl 0.15 using the spatial scheme proposed by Lockard et al. coupled with the optimised time discretisation designed by Tam and Webb

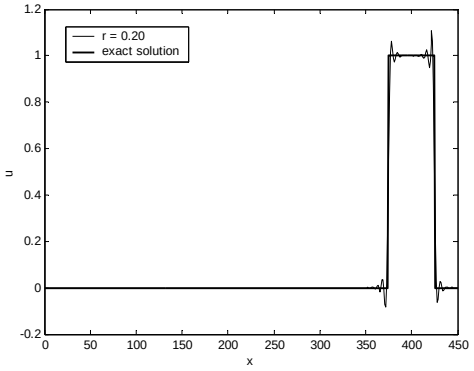

Fig. 11d Propagation of Boxcar function at dimensionless time, t=400 at cfl 0.20 using the spatial scheme proposed by Lockard et al. coupled with the optimised time discretisation designed by Tam and Webb

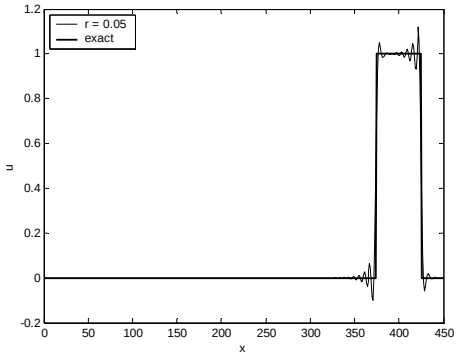

Fig. 12a Propagation of Boxcar function at dimensionless time, t=400 at cfl 0.05 using the spatial scheme proposed by Zingg et al. coupled with the optimised time discretisation designed by Tam and Webb

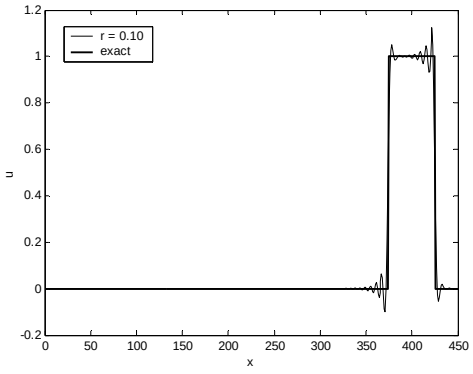

Fig. 12b Propagation of Boxcar function at dimensionless time, t=400 at cfl 0.10 using the spatial scheme proposed by Zingg et al. coupled with the optimised time discretisation designed by Tam and Webb

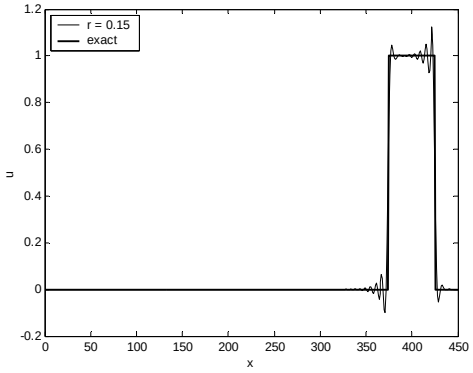

Fig. 12c Propagation of Boxcar function at dimensionless time, t=400 at cfl 0.15 using the spatial scheme proposed by Zingg et al. coupled with the optimised time discretisation designed by Tam and Webb

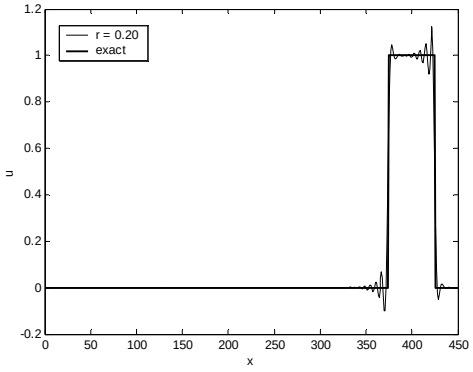

Fig. 12d Propagation of Boxcar function at dimensionless time, t=400 at cfl 0.20 using the spatial scheme proposed by Zingg et al. coupled with the optimised time discretisation designed by Tam and Webb

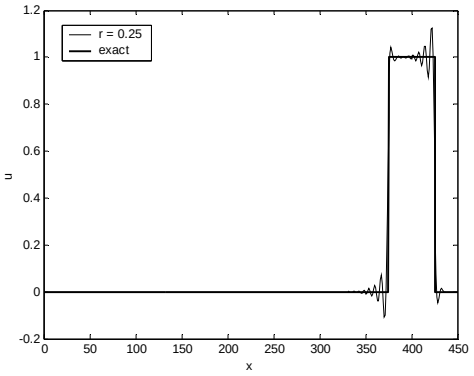

Fig. 12e Propagation of Boxcar function at dimensionless time, t=400 at cfl 0.25 using the spatial scheme proposed by Zingg et al. coupled with the optimised time discretisation designed by Tam and Webb

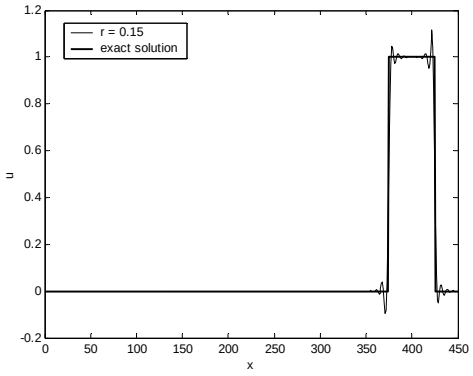

Fig. 13c Propagation of Boxcar function at dimensionless time, t=400 at cfl 0.15 using the spatial scheme proposed by Zhuang and Chen coupled with the optimised time discretisation designed by Tam and Webb

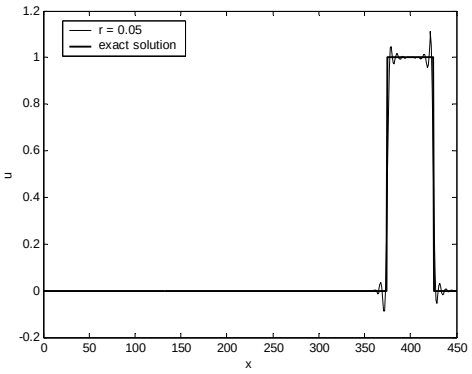

Fig. 13a Propagation of Boxcar function at dimensionless time, t=400 at cfl 0.05 using the spatial scheme proposed by Zhuang and Chen coupled with the optimised time discretisation designed by Tam and Webb

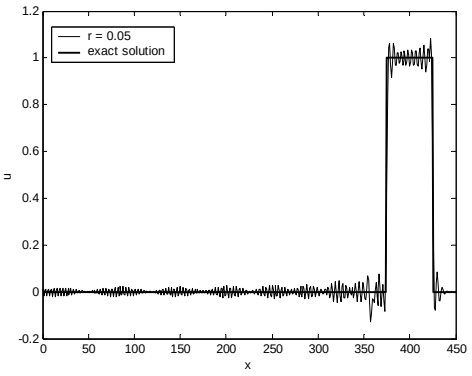

Fig. 14a Propagation of Boxcar function at dimensionless time, t=400 at cfl 0.05 using the spatial scheme proposed by Bogey and Bailly coupled with the optimised time discretisation designed by Tam and Webb

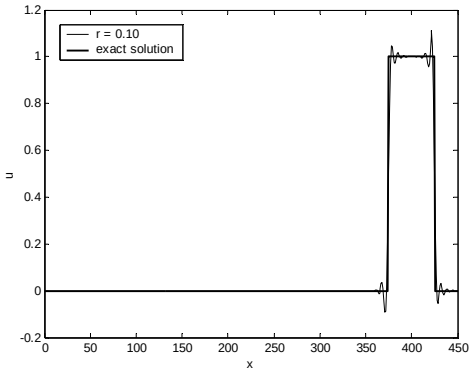

Fig. 13b Propagation of Boxcar function at a dimensionless time, t=400 at cfl 0.10 using the spatial scheme proposed by Zhuang and Chen coupled with the optimised time discretisation designed by Tam and Webb

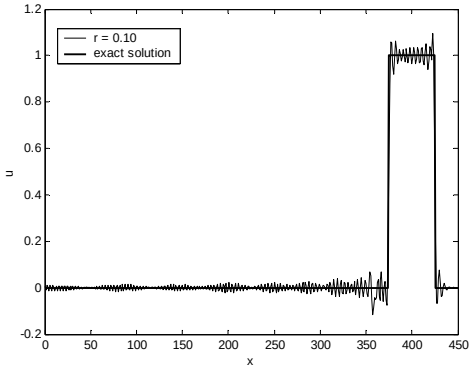

Fig. 14b Propagation of Boxcar function at dimensionless time, t=400 at cfl 0.10 using the spatial scheme proposed by Bogey and Bailly coupled with the optimised time discretisation designed by Tam and Webb

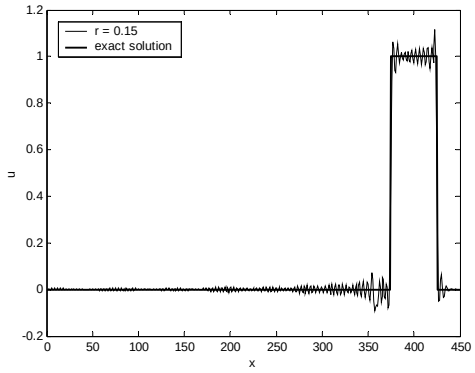

Fig. 14c Propagation of Boxcar function at a dimensionless time, t=400 at cfl 0.15 using the spatial scheme proposed by Bogey and Bailly coupled with the optimised time discretisation designed by Tam and Webb

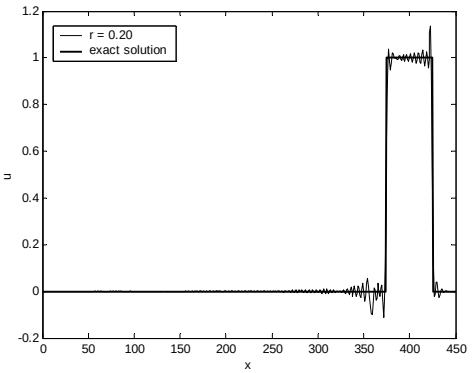

Fig. 14d Propagation of Boxcar function at a dimensionless time, t=400 at cfl 0.20 using the spatial scheme proposed by Bogey and Bailly coupled with the optimised time discretisation designed by Tam and Webb

We quantify the errors in the numerical results according to a technique devised by Takacs [21]. Based on Tables III to IX, it is observed that when the total error is least at a particular *cfl* number, at the same time, the quantity, **eeldld** is also least. The ST7 and those schemes proposed by Tam and Webb and by Zhuang and Chen coupled with a time derivative designed by Tam and Webb are most effective at cfl numbers close to 0.15. In the case of ST9, Lockard et al. and Bogey and Bailly, the optimal *cfl* is close to 0.20. The scheme proposed by Zingg et al. is optimised at a *cfl* close to 0.05.

TABLE III
QUANTIFYING DISSIPATION AND DISPERSION ERRORS FROM SOLUTIONS OF BOXCAR PROPAGATION MODELED USING THE ST7 SCHEME COUPLED WITH THE OPTIMISED TIME DISCRETISATION DESIGNED BY TAM AND WEBB

cfl	Dissipation error $/\times 10^{-6}$	Dispersion error $/\times 10^{-3}$	Total error $/\times 10^{-3}$	**eeldld** $/\times 10^{-3}$
0.05	2.160407	2.556805	2.558965	5.120152
0.10	2.314094	2.536655	2.538969	5.079750
0.15	2.665509	2.464418	2.467084	4.934914
0.20	3.429495	2.531297	2.534727	5.069007
0.25	4.662076	2.557502	2.562164	5.121550

TABLE IV
QUANTIFYING DISSIPATION AND DISPERSION ERRORS FROM SOLUTIONS OF BOXCAR PROPAGATION MODELED USING THE ST9 SCHEME COUPLED WITH THE OPTIMISED TIME DISCRETISATION DESIGNED BY TAM AND WEBB

cfl	Dissipation error/ $\times 10^{-5}$	Dispersion error/ $\times 10^{-2}$	Total error/ $\times 10^{-2}$	**eeldld** $/\times 10^{-2}$
0.05	1.140688	2.750905	2.752046	5.578184
0.10	1.105151	2.695485	2.696590	5.464284
0.15	1.097861	2.667495	2.668593	5.406782
0.20	1.141162	2.565923	2.567065	5.198252

TABLE V
QUANTIFYING DISSIPATION AND DISPERSION ERRORS FROM SOLUTIONS OF BOXCAR PROPAGATION MODELED USING THE SPATIAL DISCRETISATION COUPLED WITH THE OPTIMISED TIME DISCRETISATION DESIGNED BY TAM AND WEBB

cfl	Dissipation error $/\times 10^{-6}$	Dispersion error / $\times 10^{-3}$	Total error / $\times 10^{-3}$	**eeldld** $/\times 10^{-3}$
0.05	2.045489	1.714735	1.716781	3.432412
0.10	2.210867	1.657635	1.659846	3.318019
0.15	2.596401	1.584709	1.587305	3.171931
0.20	3.414697	1.603478	1.606892	3.209528

TABLE VI
QUANTIFYING DISSIPATION AND DISPERSION ERRORS FROM SOLUTIONS OF BOXCAR PROPAGATION MODELED USING THE SPATIAL DISCRETISATION OF LOCKARD ET AL. COUPLED WITH THE OPTIMISED TIME DISCRETISATION DESIGNED BY TAM AND WEBB

cfl	Dissipation error $/\times 10^{-5}$	Dispersion error $/\times 10^{-3}$	Total error $/\times 10^{-3}$	**eeldld** $/\times 10^{-3}$
0.05	2.071901	1.382941	1.403660	2.767796
0.10	1.919610	1.312450	1.331646	2.626624
0.15	1.770409	1.279176	1.296880	2.559989
0.20	1.637648	1.247946	1.264323	2.497450

TABLE VII
QUANTIFYING DISSIPATION AND DISPERSION ERRORS FROM SOLUTIONS OF BOXCAR PROPAGATION [19] MODELED USING THE SPATIAL DISCRETISATION OF ZINGG ET AL. COUPLED WITH THE OPTIMISED TIME DISCRETISATION DESIGNED BY TAM AND WEBB

cfl	Dissipation error $/\times 10^{-6}$	Dispersion error $/\times 10^{-3}$	Total error $/\times 10^{-3}$	**eeldld** $/\times 10^{-3}$
0.05	4.795034	1.498266	1.50306	2.998778
0.10	5.215704	1.518621	1.523837	3.039549
0.15	5.663652	1.514522	1.520186	3.031339
0.20	6.188563	1.616254	1.622443	3.235121
0.25	6.902871	1.720093	1.726995	3.443146

TABLE VIII
QUANTIFYING DISSIPATION AND DISPERSION ERRORS FROM SOLUTIONS OF BOXCAR PROPAGATION [19] MODELED USING THE SPATIAL DISCRETISATION OF ZHUANG AND CHEN COUPLED WITH THE OPTIMISED TIME DISCRETISATION DESIGNED BY TAM AND WEBB

cfl	Dissipation error $/\times 10^{-5}$	Dispersion error $/\times 10^{-3}$	Total error $/\times 10^{-3}$	**eeldld** $/\times 10^{-3}$
0.05	2.346288	1.473060	1.496523	2.948291
0.10	2.168320	1.426275	1.447958	2.854586
0.15	1.992908	1.404311	1.424240	2.810596

TABLE IX
QUANTIFYING DISSIPATION OND DISPERSION ERRORS FROM SOLUTIONS OF BOXCAR PROPAGATION [19] MODELED USING THE SPATIAL DISCRETISATION OF BOGEY AND BAILLY COUPLED WITH THE OPTIMISED TIME DISCRETISATION DESIGNED BY TAM AND WEBB

cfl	Dissipation error $/\times 10^{-5}$	Dispersion error $/\times 10^{-3}$	Total error $/\times 10^{-3}$	**eeldld** $/\times 10^{-3}$
0.05	1.139693	1.422212	1.433609	2.869274
0.10	1.100064	1.295012	1.306013	2.591702
0.15	1.094133	1.199335	1.210276	2.400109
0.20	1.136627	1.181182	1.192548	2.363760

Initial disturbance consisting of sine and gaussian functions [11]

The numerical experiment involves the long-range propagation of one-dimensional disturbance, allowing the observation of dispersion or dissipation errors. Initial disturbances at t=0 are defined by

$$u(x) = \sin\left(\frac{2\pi x}{a\Delta x}\right)\exp\left(-\ln(2)\left(\frac{x}{b\Delta x}\right)^2\right), \qquad (3)$$

where $a\Delta x$ is the dominant wavelength and $b\Delta x$ the half-width of the Gaussian function. The parameters a and b affect the spectral contents of the disturbance. In this problem, we set a=8 and b=3.

The initial perturbation is characterised by wavenumbers in the range $0 < \theta h < \frac{\pi}{2}$ with a peak for $\theta h = \frac{\pi}{4}$, i.e., for eight points per wavelength.

We obtain the numerical solution after the initial disturbance has propagated over $800\Delta x$ corresponding to 100 times the dominant wavelength, in order to stress the possible numerical numerical errors. The numerical results when solved using spatial schemes proposed by Tam and Webb [19], Lockard et al. [14], Zingg et al. [25], Zhuang and Chen [26], Bogey and Bailly [8], all combined with the time derivative designed by Tam and Webb are illustrated in Figs. (15) to (19).

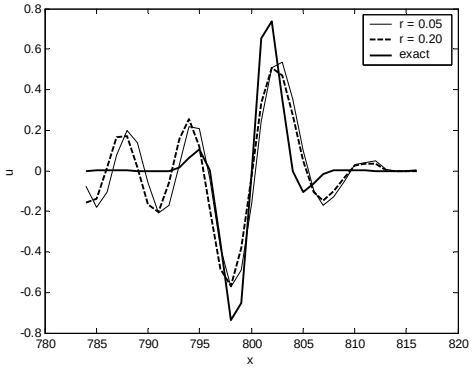

Fig. 15 Solution for one-dimensional disturbance at dimensionless time, t=800 at 2 different cfl numbers using the spatial scheme coupled with the optimised time discretisation designed by Tam and Webb (DRP scheme)

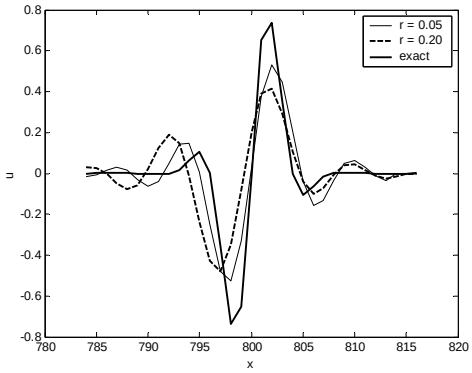

Fig. 16 Solution for one-dimensional disturbance at dimensionless time, t=800 at 2 different cfl numbers using the spatial scheme proposed by Lockard et al. [14] coupled with the optimised time discretisation designed by Tam and Webb

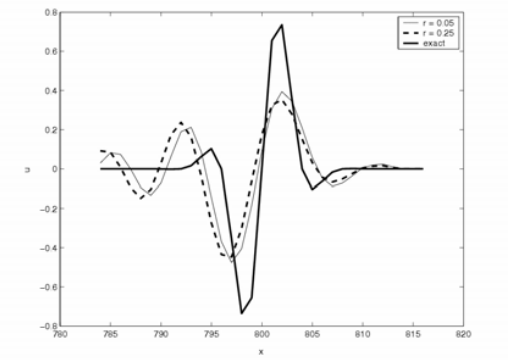

Fig. 17 Solution for one-dimensional disturbance at dimensionless time, t=800 at 2 different cfl numbers using the spatial scheme proposed by Zingg et al. [24] coupled with the optimised time discretisation designed by Tam and Webb

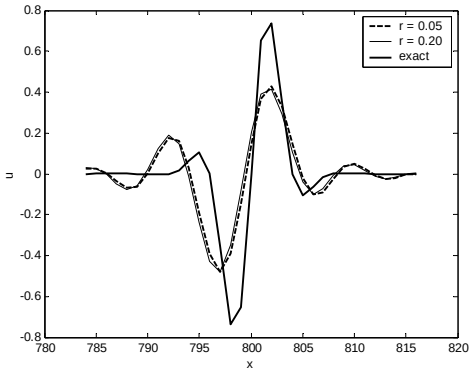

Fig. 18 Solution for one-dimensional disturbance at dimensionless time, t=800 at 2 different cfl numbers using the spatial scheme proposed by Zhuang and Chen [26] coupled with the optimised time discretisation designed by Tam and Webb

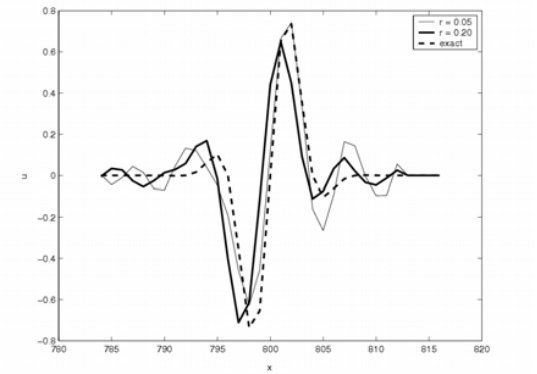

Fig. 19 Solution for one-dimensional disturbance at dimensionless time, t=800 at 2 different cfl numbers using the spatial scheme proposed by Bogey and Bailly [8] coupled with the optimised time discretisation designed by Tam and Webb

TABLE X
QUANTIFYING DISSIPATION AND DISPERSION ERRORS FROM SOLUTIONS OF THE LONG-RANGE PROPAGATION OF ONE-DIMENSIONAL DISTURBANCE USING SPATIAL SCHEME COUPLED WITH THE OPTIMISED TIME DISCRETISATION DESIGNED BY TAM AND WEBB [19] (DRP SCHEME)

cfl	Dissipation error	Dispersion Error $/\times 10^{-3}$	Total Error $/\times 10^{-3}$	**eeldld** $/\times 10^{-3}$
0.05	8.166709 $\times 10^{-10}$	1.399802	1.399803	2.801564
0.10	9.171561 $\times 10^{-10}$	1.349753	1.349754	2.701328
0.15	3.115731 $\times 10^{-7}$	1.248022	1.248333	2.497602
0.20	7.875999 $\times 10^{-6}$	1.122106	1.129982	2.245472

TABLE XI
QUANTIFYING DISSIPATION AND DISPERSION ERRORS FROM SOLUTIONS OF THE LONG-RANGE PROPAGATION OF ONE-DIMENSIONAL DISTURBANCE USING SPATIAL SCHEME OF LOCKARD ET AL. [14] COUPLED WITH THE OPTIMISED TIME DISCRETISATION DESIGNED BY TAM AND WEBB [19]

cfl	Dissipation Error	Dispersion Error $/\times 10^{-4}$	Total Error $/\times 10^{-4}$	**eeldld**
0.05	9.740815 $\times 10^{-5}$	4.714690	5.688771	9.43170 $\times 10^{-4}$
0.10	9.685720 $\times 10^{-5}$	4.908912	5.877484	9.82033 $\times 10^{-4}$
0.15	9.731555 $\times 10^{-5}$	5.761992	6.735148	1.152740 $\times 10^{-3}$
0.20	1.047971 $\times 10^{-4}$	7.140597	8.188568	1.428640 $\times 10^{-3}$

TABLE XII
QUANTIFYING DISSIPATION AND DISPERSION ERRORS FROM SOLUTIONS OF THE LONG-RANGE PROPAGATION OF ONE-DIMENSIONAL DISTURBANCE USING SPATIAL SCHEME OF ZINGG ET AL. [24] COUPLED WITH THE OPTIMISED TIME DISCRETISATION DESIGNED BY TAM AND WEBB [19]

cfl	Dissipation error $/\times 10^{-4}$	Dispersion error $/\times 10^{-3}$	Total error $/\times 10^{-3}$	**eeldld** $/\times 10^{-3}$
0.05	1.999592	1.005770	1.205729	2.012592
0.10	1.986953	1.051157	1.249852	2.011282
0.15	1.986153	1.165015	1.363630	2.331427
0.20	2.038447	1.262122	1.465967	2.525879
0.25	2.245064	1.465909	1.690415	2.934018

TABLE XIII
QUANTIFYING DISSIPATION AND DISPERSION ERRORS FROM SOLUTIONS OF THE LONG-RANGE PROPAGATION OF ONE-DIMENSIONAL DISTURBANCE USING SPATIAL SCHEME OF ZHUANG ET AL. [26] COUPLED WITH THE OPTIMISED TIME DISCRETISATION DESIGNED BY TAM AND WEBB [19]

cfl	Dissipation Error $/\times 10^{-4}$	Dispersion Error $/\times 10^{-4}$	Total Error $/\times 10^{-3}$	**eeldld** $/\times 10^{-3}$
0.05	2.004390	9.386854	1.137124	1.878292
0.10	1.991618	9.963253	1.195487	1.993683
0.15	1.989300	1.144283	1.343213	2.289916

TABLE XIV
QUANTIFYING DISSIPATION AND DISPERSION ERRORS FROM SOLUTIONS OF THE LONG-RANGE PROPAGATION OF ONE-DIMENSIONAL DISTURBANCE USING SPATIAL SCHEME OF BOGEY AND BAILLY [8] COUPLED WITH THE OPTIMISED TIME DISCRETISATION DESIGNED BY TAM AND WEBB [19]

cfl	Dissipation error	Dispersion error	Total error	**eeldld**
0.05	9.246997 $\times 10^{-10}$	3.979900 $\times 10^{-4}$	3.979909 $\times 10^{-4}$	7.96138 $\times 10^{-4}$
0.10	5.614171 $\times 10^{-10}$	4.49797 $\times 10^{-4}$	4.490803 $\times 10^{-4}$	8.98361 $\times 10^{-4}$
0.15	3.565916 $\times 10^{-7}$	6.921090 $\times 10^{-4}$	6.924656 $\times 10^{-4}$	1.384697 $\times 10^{-3}$
0.20	8.195438 $\times 10^{-6}$	1.228249 $\times 10^{-3}$	1.236444 $\times 10^{-3}$	2.458007 $\times 10^{-3}$

Tables X to XIV show that in the case of the long-range propagation of the 1-D disturbance, both the total error and the quantity, eeldld are both least at the same cfl number for a numerical method approximating the linear advection equation, under consideration. The scheme proposed by Tam and Webb [19] is most effective at a cfl close to 0.20. On the other hand, the methods proposed by Lockard et al, [14], Zingg et al. [24], Zhuang and Chen [26], Bogey and Bailly [8] when coupled with the optimized time derivative designed by Tam and Webb are all most effective at cfl numbers close to 0.05.

Initial disturbance consisting of Gaussian profile [12,15]

We consider the following problem

$$u(x, t = 0) = 0.5 \exp\left(- \ln(2)\left(\frac{x}{b}\right)^2 \right) \quad (4)$$

We present the results using the spatial derivatives proposed by Tam and Webb [19] and by Bogey and Bailly [8]. Also, three categories of waves are considered namely;
1) short waves (b = 3)
2) intermediate waves (b = 6)
3) long waves (b = 20).

The results are displayed in Figs.(20) to (27) and the errors tabulated in Tables XV to XX.

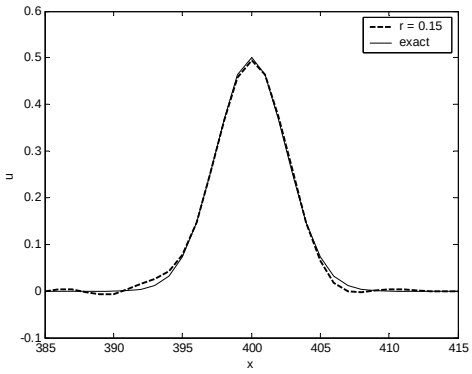

Fig. 20 Solution for initial disturbance consisting of a Gaussian profile at dimensionless time, t=400 using the DRP scheme [19] at cfl number 0.15, with b = 3

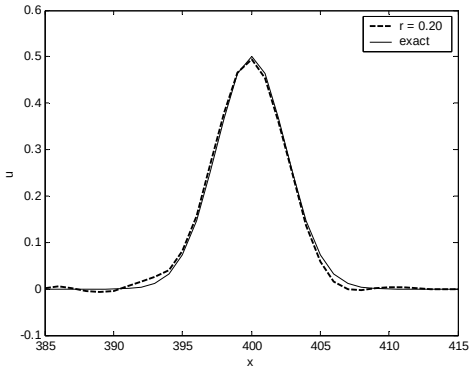

Fig. 21 Solution for initial disturbance consisting of a Gaussian profile at dimensionless time, t=400 using the DRP scheme [19] at cfl number 0.20, with b = 3

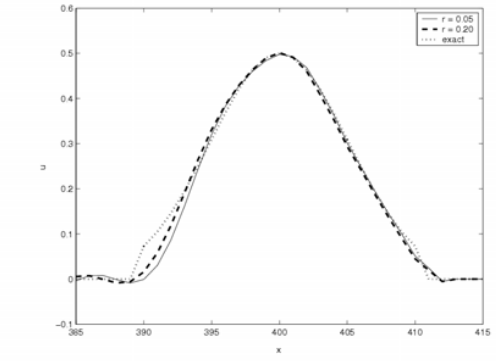

Fig. 22 Solution for initial disturbance consisting of a Gaussian profile at dimensionless time, t=400 using the DRP scheme [19], with b = 6

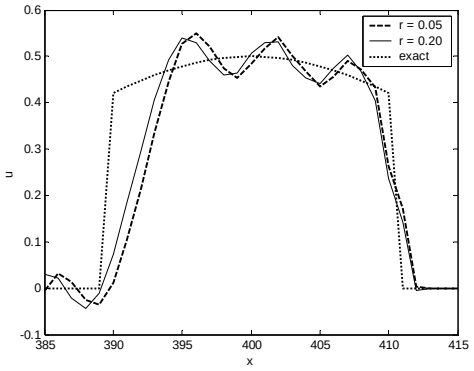

Fig. 23 Solution for initial disturbance consisting of a Gaussian profile at dimensionless time, t=400 using the DRP scheme [19], with b = 20

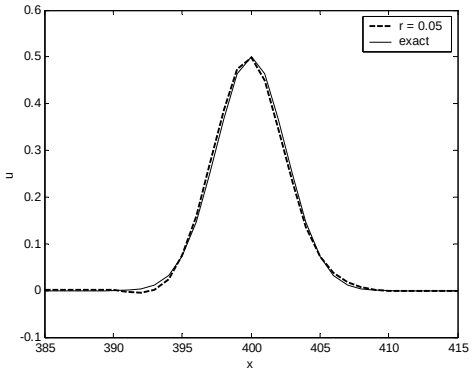

Fig. 24 Solution for initial disturbance consisting of a Gaussian profile at dimensionless time, t=400 using the spatial discretisation proposed by Bogey and Bailly [8] coupled with the optimized time discretisation designed by Tam and Webb [19] at cfl=0.05, with b = 3

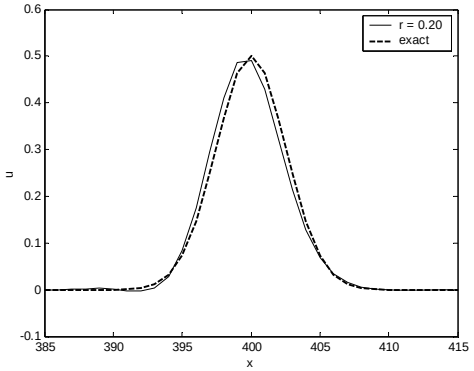

Fig. 25 Solution for initial disturbance consisting of a Gaussian profile at dimensionless time, t=400 using the spatial discretisation proposed by Bogey and Bailly [8] coupled with the optimised time discretisation designed by Tam and Webb [19] at cfl=0.20, with b = 3

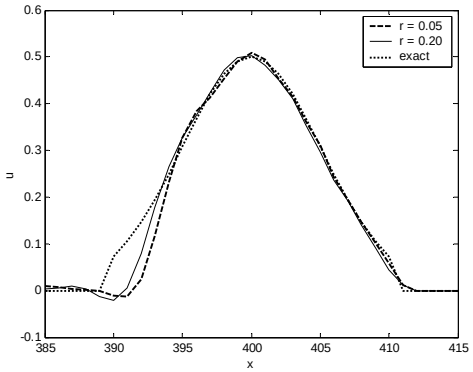

Fig. 26 Solution for initial disturbance consisting of a Gaussian profile at dimensionless time, t=400 using the spatial discretisation proposed by Bogey and Bailly [8] coupled with the optimized time discretisation designed by Tam and Webb [19], with b = 6

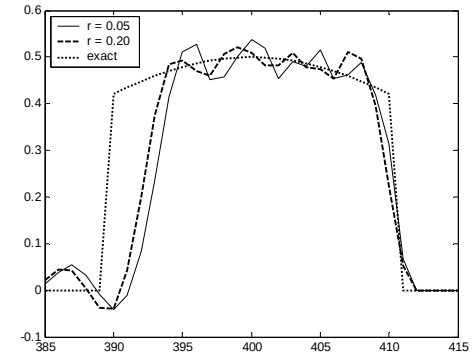

Fig. 27 Solution for initial disturbance consisting of a Gaussian profile at dimensionless time, t=400 using the spatial discretisation proposed by Bogey and Bailly [8] coupled with the optimised time discretisation designed by Tam and Webb [19] with b = 20

TABLE XV
QUANTIFYING DISSIPATION AND DISPERSION ERRORS FROM SOLUTIONS OF THE GAUSSIAN PROPAGATION OF USING THE SPATIAL SCHEME COUPLED WITH THE OPTIMISED TIME DISCRETISATION DESIGNED BY TAM AND WEBB [19], WITH B = 3

cfl	Dissipation error	Dispersion error $/\times 10^{-6}$	Total error $/\times 10^{-6}$	**eeldld** $/\times 10^{-6}$
0.05	2.432768 $\times 10^{-11}$	4.821456	4.821480	9.642
0.10	1.186329 $\times 10^{-11}$	3.531614	3.531626	7.064
0.15	6.595188 $\times 10^{-12}$	3.105185	3.105191	6.210
0.20	2.703211 $\times 10^{-11}$	4.988251	4.988278	9.976

TABLE XVI
QUANTIFYING DISSIPATION AND DISPERSION ERRORS FROM SOLUTIONS OF THE GAUSSIAN PROPAGATION OF USING SPATIAL SCHEME COUPLED WITH THE OPTIMISED TIME DISCRETISATION DESIGNED BY TAM AND WEBB [19], WITH $B = 6$

cfl	Dissipation error $/\times 10^{-7}$	Dispersion error $/\times 10^{-5}$	Total error	**eeldld** $/\times 10^{-5}$
0.05	5.481085	4.665514	4.720325 $\times 10^{-4}$	9.3312
0.10	4.334617	3.817972	3.861318 $\times 10^{-5}$	7.6361
0.15	3.402044	3.190306	3.224326 $\times 10^{-5}$	6.3807
0.20	2.676630	2.522800	2.549567 $\times 10^{-5}$	5.0457

TABLE XVII
QUANTIFYING DISSIPATION AND DISPERSION ERRORS FROM SOLUTIONS OF THE GAUSSIAN PROPAGATION OF USING SPATIAL SCHEME COUPLED WITH THE OPTIMISED TIME DISCRETISATION DESIGNED BY TAM AND WEBB [19], WITH $B = 20$

cfl	Dissipation error $/\times 10^{-5}$	Dispersion error	Total error	**eeldld** $/\times 10^{-3}$
0.05	3.979960	1.089400 $\times 10^{-3}$	1.129199 $\times 10^{-3}$	2.179988
0.10	3.477232	9.754649 $\times 10^{-4}$	1.010237 $\times 10^{-3}$	1.951883
0.15	3.103162	8.713757 $\times 10^{-4}$	9.024073 $\times 10^{-4}$	1.743512
0.20	2.883936	7.119052 $\times 10^{-4}$	7.407446 $\times 10^{-4}$	1.424318

TABLE XVIII
QUANTIFYING DISSIPATION AND DISPERSION ERRORS FROM SOLUTIONS OF THE GAUSSIAN PROPAGATION OF USING SPATIAL SCHEME OF BOGEY AND BAILLY COUPLED WITH THE OPTIMISED TIME DISCRETISATION DESIGNED BY TAM AND WEBB [19], WITH $B = 3$

cfl	Dissipation error	Dispersion error	Total error	**eeldld** $/\times 10^{-5}$
0.05	3.599248 $\times 10^{-10}$	5.630459 $\times 10^{-6}$	5.630819 $\times 10^{-6}$	1.1261
0.10	2.037520 $\times 10^{-10}$	9.602210 $\times 10^{-6}$	9.602413 $\times 10^{-6}$	1.9204
0.15	1.064683 $\times 10^{-10}$	1.078054 $\times 10^{-5}$	1.078065 $\times 10^{-5}$	2.1561
0.20	7.078462 $\times 10^{-11}$	2.443306 $\times 10^{-5}$	2.443313 $\times 10^{-5}$	4.8866

TABLE XIX
QUANTIFYING DISSIPATION AND DISPERSION ERRORS FROM SOLUTIONS OF THE GAUSSIAN PROPAGATION OF USING SPATIAL SCHEME OF BOGEY AND BAILLY COUPLED WITH THE OPTIMISED TIME DISCRETISATION DESIGNED BY TAM AND WEBB [19], WITH $B = 6$

cfl	Dissipation error	Dispersion error	Total error	**eeldld** $/\times 10^{-4}$
0.05	1.762725 $\times 10^{-6}$	1.048510 $\times 10^{-4}$	1.066138 $\times 10^{-4}$	2.09713
0.10	1.432981 $\times 10^{-6}$	8.942894 $\times 10^{-5}$	9.086193 $\times 10^{-5}$	1.78866
0.15	1.174016 $\times 10^{-6}$	7.763200 $\times 10^{-5}$	7.880602 $\times 10^{-5}$	1.55270
0.20	9.707269 $\times 10^{-7}$	6.205850 $\times 10^{-5}$	6.302923 $\times 10^{-5}$	1.24121

TABLE XX
QUANTIFYING DISSIPATION AND DISPERSION ERRORS FROM SOLUTIONS OF THE GAUSSIAN PROPAGATION OF USING SPATIAL SCHEME OF BOGEY AND BAILLY COUPLED WITH THE OPTIMISED TIME DISCRETISATION DESIGNED BY TAM AND WEBB [19], WITH $B = 20$

cfl	Dissipation error $/\times 10^{-5}$	Dispersion error $/\times 10^{-3}$	Total error $/\times 10^{-3}$	**eeldld** $/\times 10^{-3}$
0.05	7.737032	1.474945	1.552316	2.952073
0.10	6.995402	1.363594	1.433548	2.729053
0.15	6.513239	1.254267	1.319399	2.510112
0.20	6.192883	1.100220	1.162149	2.201654

Based on the values of **eeldld**, it is concluded that the DRP scheme is most effective at cfl close to 0.15 to model the propagation of the gaussian function with $b = 3$. For other values of b, such as 6 and 20, the optimal cfl is 0.20. Considering the method based on the spatial discretisation proposed by Bogey and Bailly [8] and the temporal discretisation proposed by Tam and Webb [19], with reference to the eeldld values, we deduce that for $b = 3$, the optimal cfl is close to 0.05 but for other types of waves ($b = 6$, $b = 20$), the most suitable value of the cfl is close to 0.20.

II. CONCLUSION

In this work, we have combined some spatial derivatives with the optimised time derivative derived by Tam and Webb [19] to obtain seven different multi-level finite difference schemes. We have also analysed the variation of the modified wavenumber and group velocity, both with respect to the exact wavenumber for each of the seven spatial derivatives used. The problems solved deal with the 1-D wave propagation like the Boxcar function, an initial disturbance containing sine and gaussian functions and the propagation of a gaussian profile with three categories of waves considered. We have quantified the dissipation and dispersion errors from the numerical results obtained at some different cfl numbers. Based on the numerical experiments solved using a given

optimised numerical method, it can seen that the results are dependent on the type of waves which are simulated and also on the Courant number used.

ACKNOWLEDGMENT

Mr. Appadu is a Phd student at the University of Mauritius (UOM) and has been partially supported by the Tertiary Education Commission (TEC) and the UOM for the research through a bursary.

REFERENCES

[1] A.R. Appadu, M.Z. Dauhoo and S.D.D.V. Rughooputh. Optimisation of Numerical Schemes Using the Minimised Integrated Square Difference Error. Research and Innovation Challenges. University of Mauritius, 16-20 January 2007.
[2] A.R. Appadu, M.Z. Dauhoo and S.D.D.V. Rughooputh. Control of Numerical Effects of Dispersion and Dissipation in Numerical Schemes for Efficient Shock-Capturing Through an Optimal Courant Number. Computers and Fluids, Vol. 37, No. 6, 2008, pp. 767-783.
[3] A.R. Appadu and M.Z. Dauhoo. A Note on the Two Versions of Lax-Friedrichs Scheme. Proceedings of The 2007 International Conference on Scientific Computing. CSREA Press, Editors: H. R. Arabnia and J. Y. Yang and M. Q. Yang.
[4] A.R. Appadu, M.Z. Dauhoo and S.D.D.V. Rughooputh. Efficient Shock-Capturing Numerical Schemes Using the Approach of Minimised Integrated Square Difference Error for Hyperbolic Conservation Laws. Proceedings of Computational Science and Its Applications- ICCSA 2007. Lecture Notes in Computer Science. Editors: O. Gervasi Osvaldo and M.L. Gavrilova, Vol. III.
[5] A.R. Appadu and M.Z. Dauhoo. On the Concept of Minimised Integrated Square Difference Error: Its Mechanism and Some of Its Applications. Submitted to SIAM Journal of Numerical Analysis (September 2008).
[6] A.R. Appadu and M.Z. Dauhoo. The Concept of Minimised Integrated Exponential Error for Low Dispersion and Low Dissipation. Submitted to International Journal for Numerical Methods in Fluids (September 2008).
[7] G. Ashcroft and X. Zhang. Optimised prefactored compact schemes, Journal of Computational Physics, vol. 190, 2003, pp. 459-477.
[8] C. Bogey and C. Bailly. A Family of Low Dispersive and Low Dissipative Explicit Schemes for Computing the Aerodynamic Noise. AIAA-Paper 2002.
[9] C. Bogey and C. Bailly. A Family of Low Dispersive and Low Dissipative Explicit Schemes for Flow and Noise Computations. Journal of Computational Physics, 2004, vol. 194, pp. 194-214.
[10] Lodovica Ferraria. http://www.sosmath.com/algebra/factor/fac12/fac12.html.
[11] R. Hixon. Evaluation of high-accuracy MacCormack-Type scheme using Benchmark Problems, NASA Contractor Report 202324, ICOMP-97-03-1997.
[12] F.Q. Hu, M.Y. Hussaini and J. Manthey. Low-Dissipation and Dispersion Runge-Kutta Schemes For Computational Acoustics. Technical Report: TR-94-102, 1994.
[13] S. Johansson. High Order Finite Difference Operators with the Summation by Parts Property based on DRP Schemes, Division of Scientific Computing-Department of Information Technology, Uppsala University, Sweden, 2007.
[14] D.P. Lockard, K.S. Brentner and H.L. Atkins. High-accuracy algorithms for computational aeroacoustics. AIAA Journal, vol. 33, No. 2, pp. 246-251, 1995.
[15] M. Popescu and W. Shyy. Dispersion-Relation-Preserving and Space-Time schemes for Wave Equations, AIAA, Paper No. 202-0225, 2002.
[16] P. Roe. Linear Bicharacteristics schemes without dissipation. SIAM Journal of Scientific Computing, vol. 19, No. 5, (1998), pp. 1405-1429.
[17] W. De Roeck, M. Baelmans, and P. Sas. An overview of high-order finite difference schemes for computational aeroacoustics, International Conference on Noise and Vibration Engineering. Katholieke Universiteit Leuven, Belgium, ISMA 20-22 September 2004, pp. 353-368.
[18] T.K. Sengupta, G. Ganeriwal and S. De. Analysis of Central and Upwind Compact Schemes. Journal of Computational Physics, Vol. 192, 2003, pp. 677-694.
[19] C.K.W. Tam and J.C. Webb. Dispersion-Relation-Preserving Finite Difference Schemes for Computational Acoustics. Journal of Computational Physics, Vol. 107, 1993, pp. 262-281.
[20] C.K.W. Tam. Computational Aeroacoustics: Issues and Methods. AIAA, 33, 10, pp. 1788-1796, October 1995.
[21] L. Takacs. A Two-step scheme for the Advection Equation with Minimized Dissipation and Dispersion errors. Monthly Weather Review. 113, (1985), pp. 1050-1065.
[22] D. J. Webb, B.A. De Cuevas and C.S. Richmond. Improved Advection Schemes for Ocean Models. Journal of Atmospheric and Oceanic Technology. Vol. 15, No. 5, 1998, pp. 1171-1187.
[23] V.L.Wells and R.A.Renault. Computing Aerodynamically Generated Noise, Annual Rev. Fluid Mechanics, vol. 29, 1997, pp.161-199.
[24] D.W. Zingg, H. Lomax and H.M. Jurgens. High-Accuracy finite difference schemes for linear wave propagation. SIAM Journal of Scientific Computing, vol. 17, no. 2, 1996, pp. 328-346.
[25] D.W. Zingg. Comparison of High-Accuracy Finite-Difference Methods for Linear Wave Propagation. SIAM Journal of Scientific Computing. Vol. 22,no. 2, pp. 476-502, 2001.
[26] M. Zhuang and R.F. Chen. Application of high-order optimised upwind schemes for computational aeroacoustics. AIAA Journal, vol. 40,No. 3, 2002, pp. 443-449.